Astron. Astrophys. 264, 489–492 (1992)

ASTRONOMY AND ASTROPHYSICS

Radio structure of the Seyfert galaxy Markarian 509

K.P. Singh[1] **and N.J. Westergaard**[2]

[1] Tata Institute of Fundamental Research, Homi Bhabha Road, Bombay 400005, India
[2] Danish Space Research Institute, Lundtoftevej 7, Lyngby, DK-2800, Denmark

Received February 13, accepted May 19, 1992

Abstract. Detailed radio observations of Mkn 509, a Seyfert type I galaxy, have revealed an extended radio feature at 6 and 20 cm at a position angle of $-65°$ and pointing towards the north–west. It is remarkably well-aligned with the direction of polarized H_α emission, a disk of low-ionization narrow-line region and polarized optical to infra-red continuum indicating that both scattering and synchrotron radiation contribute to the polarized emission. A faint linear structure at 6 cm (length ≈ 2 kpc), almost parallel to the minor axis of the galaxy is tentatively identified as a "jet" and needs to be confirmed with higher resolution observations. The "jet" extends into the narrow-line region and can easily be confined by the narrow-line gas. A plausible geometry of the emission regions is presented.

Key words: galaxies: individual: Mkn 509 – galaxies: Seyfert – galaxies: radio continuum

1. Introduction

The highly luminous Seyfert type I galaxy, Markarian 509 (Mkn 509), nearly resembles a quasi-stellar object although a slightly elliptical (position angle of major axis $= 70° \pm 5°$) extended galactic component can be seen in direct photographs (Adams 1977; Bradt 1980; Phillips et al. 1983). Its major axis diameter is $\sim 34''$ and it has an axial ratio of ~ 0.85 (Dahari & DeRobertis 1988; Lawrence & Elvis 1982). A rotating disk of stars, dust and low-ionization gas, normally seen in the spiral galaxies, and an outflowing system of high ionization gas has been also detected (Phillips et al. 1983). The redshift of Mkn 509 is 0.035 and its V magnitude is 13.12 (Stein & Weedman 1976). The optical continuum and line emission are found to be variable (Phillips et al. 1983). In addition, the optical emission is found to be polarized and the position angle (PA) has been measured to be $\sim 150°$ (Martin et al. 1983; Thompson & Martin 1988). A significant variability in its polarization has also been detected by Martin et al. (1983). The Hα line emission has been found to be polarized; $0.25 \pm 0.10\%$ at a position angle of $130° \pm 11°$ (Thompson & Martin 1988). Infra-red (IR) emission from Mkn 509 has been reported by Rieke (1978). Polarized optical to near-IR emission has been studied by Brindle et al. (1990a, b), who find a rising polarization with frequency and a slight frequency dependence of position angle which is $\sim 145° \pm 10°$.

Send offprint requests to: K.P. Singh

In the ultraviolet, line emission due to C III, C IV and Mg II has been identified superposed on the continuum (Wu et al. 1983). Mkn 509 is a copious source of X-ray emission and was detected in the earliest X-ray surveys (Cooke et al. 1978). The X-ray emission is highly variable, shows a strong soft X-ray bump in its X-ray spectrum as well as 6.4 keV line emission and there is also an indication of a reflected component between 10–30 keV (see Singh et al. 1990 and references therein).

Mkn 509 is a weak radio source at 20, 6 and 2 cm wavelengths (Wilson & Meurs 1982; Ulvestad & Wilson 1984; Unger et al. 1987; Antonucci & Barvainis 1988). These observations could barely resolve any extended emission around the nuclear radio source. We have carried out detailed radio observations of this source using the Very Large Array (VLA) (Napier et al. 1983) as a part of our project to monitor the source simultaneously in radio, optical, UV and X-ray wavebands. These observations have resulted in high resolution maps at 6 and 20 cm and the discovery of some interesting anisotropic features. We present these results and discuss their importance.

2. Observations, analysis and results

The Seyfert galaxy Mkn 509 was observed in the radio at 6 cm (4885 and 4835 MHz) and 20 cm (1465 and 1515 MHz) wavelengths using the VLA. The bandwidth was 50 MHz at all the frequencies. The observations were performed on 1988 October 8 with the VLA in the D/A configuration and on 1988 October 15 in the A configuration. The effective observation times on the source were 1 h at both 6 and 20 cm on both occasions. The total span of the observations was about 3 h interspersed with short observations of the calibrators. The flux-density scale was fixed using observations of 3C286 and 2008-068 on October 8, and using 3C48 and 2008-068 on October 15. The data were edited to remove the contribution from antennas with large phase errors. The edited and calibrated data were then Fourier transformed and CLEANed (Hogbohm 1974) to produce radio maps at 6 and 20 cm. The signal-to-noise in the data was sufficient to apply the technique of self-calibration (Schwab 1980). It reduced the phase errors and led to an improvement in the dynamic range. The features discussed below were seen even without self calibration.

The final radio maps obtained using the A array are shown in Figs. 1 and 2 for the 6 and 20 cm, respectively. The clean beam size for the 6 cm map is 0.5×0.4 arcsec^2 (FWHM) with a PA $= 176.5°$. The rms noise in the map is 0.065 mJy. The outermost contour is at three times the rms value. The peak flux is 2.23 mJy and the

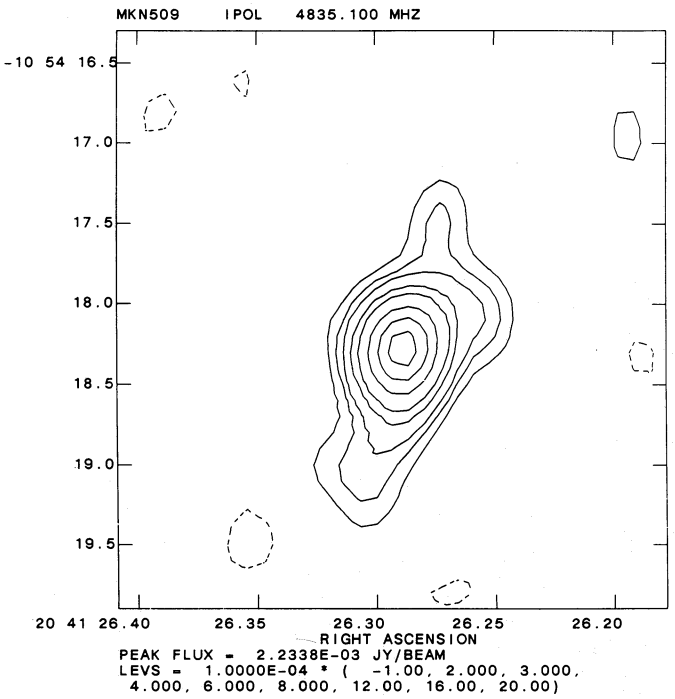

Fig. 1. Radio map of Mkn 509 at 6 cm wavelength. The beam size is $0''.5 \times 0''.4$

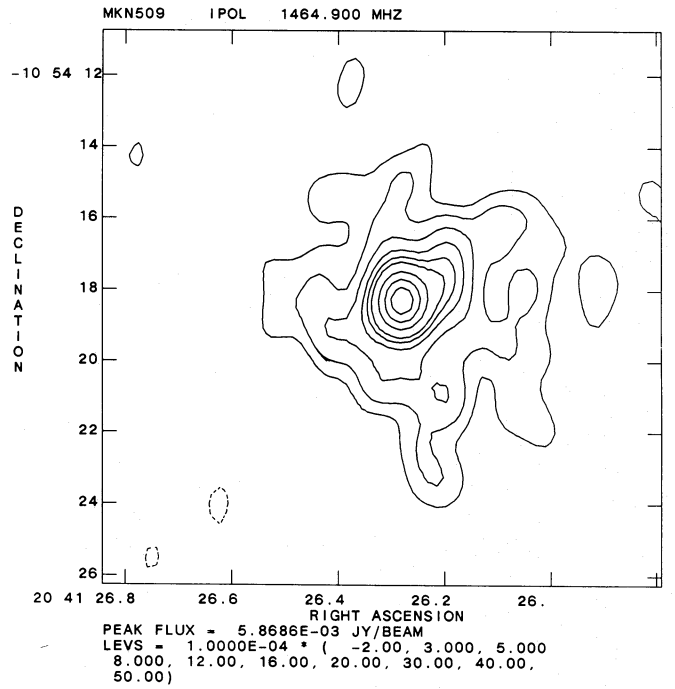

Fig. 2. Radio map of Mkn 509 at 20 cm wavelength. The beam size is $1''.5 \times 1''.1$. Please note that the scale size here is very different from that in Fig. 1.

source is clearly extended. The total flux density is 5.2 ± 0.2 mJy. An elongated structure about 2″ long is seen in the north–south direction at a position angle of $\approx 165°$. A one-sided diffuse extension (size $\approx 1''$) is also detected towards the north–west at a PA $\approx -65° \pm 5°$. The beam size for the 20 cm map is 1.5 $\times$ 1.1 arcsec^2 (FWHM) and the rms noise is 0.1 mJy. The outermost contour is at the three sigma level. The peak flux is 5.87 mJy and an amorphous extended structure (size $\approx 10'' \times 8''$) is detected. The total flux density is 24 ± 1 mJy. The most prominent elongation, extending to high intensities close to the nucleus, is towards the PAs in the range of $-40°$ to $-60°$ with the contours displaying a tendency to twist around. Extended features in the north–south direction can also be observed in the outer contours.

The beam using the D/A array was by comparison too broad to produce a good resolved image. The peak flux was found to be the same as that observed with the A array few days later and presented above.

The A array data were also examined for hourly variations in the peak flux by constructing images from observations using ~ 20 min exposures every 1 h. No variations were detected, however.

3. Discussion

The radio flux observed at 6 cm is consistent with the previous observations. The flux observed at 20 cm is, however, considerably higher. Previous observations at 20 cm with coarser resolution gave values of 12.5 ± 1 mJy (Wilson & Meurs 1982), 14 ± 2 mJy (Unger et al. 1987) and 14.8 ± 0.35 mJy (Antonucci & Barvainis 1988) and placed a limit of 1.4×0.5 arcsec^2 on its size (Unger et al. 1987). If the higher observed flux in the present observations is due to variability, one would have expected a brighter nuclear component. The unresolved nuclear source is, however, found to have a spectral index of 0.80, consistent with the previous observations (Ulvestad & Wilson 1984; Antonucci & Barvainis 1988). It seems, therefore, likely that the diffuse low-intensity extensions were not detected earlier in the less sensitive experiments.

The high resolution radio imaging has detected some very interesting features in Mkn 509 for the first time. The directions of these anisotropic emission regions are indicated schematically in Fig. 3 alongwith those of other known features in the optical to IR wavebands, and are discussed below.

3.1. Extended radio emission versus the polarized emission

As already pointed out in Sect. 2 a highly significant radio structure, though somewhat amorphous, is detected in both the 6 and 20 cm maps at a PA $= -40°$ to $-60°$ (see Figs. 1 and 2). This is aligned preferentially along the direction of the polarized optical-near IR emission (Martin et al. 1983, Brindle et al. 1990a, b) and best aligned with the direction of the Hα polarization (Thompson & Martin 1988) (see Fig. 3). This also happens to be that direction in which the disk-like rotation of the low ionization component of the extended gas in the NLR has its axis (see Phillips et al. 1983). The parallel alignment of the radio structure with the polarized optical continuum was discovered by Stockman et al. (1979) for the low polarization quasars and pointed out by Antonucci (1984) for type 1 Seyferts. The Hα polarization indicates that scattering is present and that the scattering geometry is closely related to the radio emitting region rather than the large scale optical structure. The observations, therefore, support both the presence of a polarized component due to non-thermal synchrotron radiation, dominant in the IR and radio, and another polarized component due to scattering dominant at

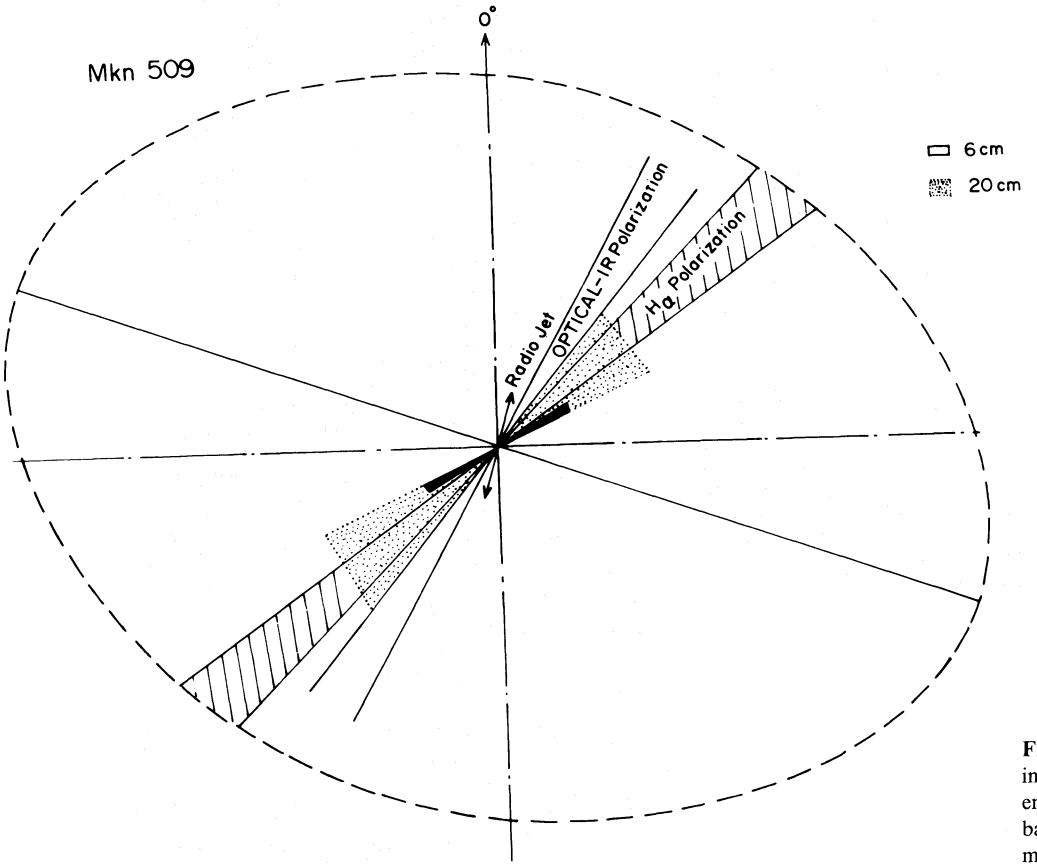

Fig. 3. Schematic diagram showing the directions of the anisotropic emission regions in different wavebands and a plausible geometrical model for them

shorter wavelengths as was first pointed out by Brindle et al. (1990b).

3.2. A radio jet?

A linear structure ($\approx$2 kpc long; $H_0 = 50$ km s^{-1} Mpc^{-1}) aligned almost perpendicular to the optical major axis of the galaxy is seen at 6 cm (Fig. 1). The surface brightness of this feature is, however, not very high. This linear structure is not resolved at 20 cm (Fig. 2), which is not very surprising given the low surface brightness of the feature and the much poorer resolution of the 20 cm map. A somewhat larger north–south extension coinciding with its direction can, however, be seen in the 20 cm map. The linear extension towards the south could then indicate either an unrelated feature in the 20 cm map or an extension with a change of direction in the south. A convolution of the 6 cm map with the resolution of the 20 cm map fails to show the inner linear structure. Higher resolution 20 cm observations are required to confirm the existence of this structure. If confirmed, a plausible interpretation for this elongation can be synchrotron emission along a collimated ejection from the nucleus in a "jet" directed along the minor axis of the galaxy. The overall shape in the bending jet scenario, however, does not resemble the usual S-shape seen in some Seyfert galaxies (Wilson & Ulvestad 1982). The transverse extension of the "jet" is unresolved and an upper limit of 0.3″ ($\approx$300 pc) is derived. By assuming that the radio emission is due to synchrotron radiation from relativistic electrons in a magnetic field, we can, by following Miley (1980), derive equipartition magnetic field and the minimum energy density in the jet. We assume that the ratio of the energy in heavy particles to that in the electrons is unity, the filling factor of the emitting region is 1, the radio spectral index is 0.8 over the frequency range of 0.01–100 GHz and that the angle between the uniform magnetic field and the line of sight is 90°. From Fig. 1 we have a flux density of 0.3 mJy in the jet, a projected size of $2'' \times 0.3''$, and assumed path length of 0.3 kpc through the jet, which give a value of $3.3\,10^{-5}$ G for the equipartition magnetic field. The corresponding minimum energy density in the relativistic particles is $\approx 10^{-10}$ erg cm^{-3} and, therefore, the relativistic particle pressure is $3.5\,10^{-11}$ dyn cm^{-2}. For a temperature of 10^4 K in the narrow line region (NLR), an electron density of >25 cm^{-3} is sufficient to confine the jet in the NLR, a requirement that is easily accommodated. Assuming that Mkn 509 emits most of its energy in X-rays and using the measured luminosity of $8.7\,10^{44}$ erg s^{-1} in the 0.1–30 keV (Singh et al. 1990) we estimate the radiation energy density of the source to be $2.4\,10^{-10}$ erg cm^{-3}. Following Miley (1980), we then derive a radiative lifetime of $\approx 3\,10^5$ yr which is comparable to the time scale for the clouds to cross the nuclear region and replenish the central source. The properties of the jet are similar to those of other Seyfert galaxies studied by Wilson & Willis (1980).

A plausible picture giving a geometrical sketch of the emitting regions in Mkn 509 is shown in Fig. 3. A relativistic jet directed along the minor axis of the galaxy punches a funnel through the interstellar medium of the galaxy. The narrow line clouds are entrained along the walls of the funnel, whose half-cone opening angle could be as large as 40°, and produce the polarized optical emission due to scattering. The synchrotron radio and IR emission is also produced along these regions. The northern end of the funnel is perhaps tilted forward, foreshortening the jet and

leading to the non-detection of the radio synchrotron emission from the other symmetrically placed regions of the funnel due to absorption and projection effects. Alternately, a spiral-like disk structure in the north–west could also be responsible for the synchrotron radiation and polarized emission due to scattering in the NLR along the disk.

High resolution optical observations with the New Technology Telescopes or the Hubble Telescope, mapping of the NLR, and radio polarization measurements would be extremely useful in further understanding of the emission mechanisms at work in Mkn 509.

Acknowledgements. We are thankful to the staff operating the VLA and for scheduling these observations at a short notice. The VLA data were analyzed at the National Centre for Image Processing at Ooty, India. We thank Chris Salter for help with the reduction and analysis of the VLA data. We are grateful to H.W. Schnopper for constant encouragment and helpful discussions. We thank A.R. Rao for useful discussions.

References

Adams T.F., 1977, ApJS 33, 19
Antonucci R., Barvainis R., 1988, ApJ 332, L13
Antonucci R.R.J., 1984, ApJ 278, 499
Bradt H.V., 1980, Ann. NY Acad. Sci. 336, 59
Brindle C., Hough J.H., Bailey J.A., Axon D.J., Ward M.J., Sparks W.B., McLean I.S., 1990a, MNRAS 244, 577
Brindle C., Hough J.H., Bailey J.A., Axon D.J., Ward M.J., Sparks W.B., McLean I.S., 1990b, MNRAS 244, 604
Cooke B.A., et al., 1978, MNRAS 182, 489
Dahari O., deRobertis, M.M., 1988, ApJS 67, 249
Hogbohm J.A., 1974, AAS 15, 417
Lawrence A., Elvis M., 1982, ApJ 256, 410
Martin P.G., Thompson I.B., Maza J., Angel J.R.P., 1983, ApJ 266, 470
Miley G., 1980, ARA&A 18, 165
Napier P.J., Thompson A.R., Ekers R.D., 1983, Proc. IEEE 71, 1295
Phillips M.M., Baldwin J.A., Atwood B., Carswell R.F., 1983, ApJ 274, 558
Rieke G.H., 1978, ApJ 226, 550
Schwab F.R., 1980, SPIE Proc. 231, 18
Singh K.P., Westergaard N.J., Schnopper H.W., Awaki H., Tawara Y., 1990, ApJ 363, 131
Stein W.A., Weedman D.W., 1976, ApJ 205, 44
Stockman H.S., Angel J.R.P., Miley G.K., 1979, ApJ 227, L55
Thompson I.B., Martin P.G., 1988, ApJ 330, 121
Ulvestad J.S., Wilson A.S., 1984, ApJ 278, 544
Unger S.W., Lawrence A., Wilson A.S., Elvis M., Wright A.E., 1987, MNRAS 228, 521
Wilson A.S., Meurs E.J.A., 1982, A&AS 50, 217
Wilson A.S., Ulvestad J.S., 1982, ApJ 263, 576
Wilson A.S., Willis A.G., 1980, ApJ 240, 429
Wu C.-C., Boggess A., Gull T.R., 1983, ApJ 266, 28